Structure and Function of Alternative Proton-Relay Mutants of Dihydrofolate Reductase[†,‡]

Cynthia L. David,[§] Elizabeth E. Howell,[∥] Martin F. Farnum,[§] J. Ernest Villafranca,[⊥] Stuart J. Oatley,[#] and Joseph Kraut*[,§]

Department of Chemistry, University of California, San Diego, La Jolla, California 92093, Department of Biochemistry, Walters Life Science Building, University of Tennessee, Knoxville, Tennessee 37996, and Agouron Pharmaceuticals Inc., 3565 General Atomics Court, San Diego, California 92121

Received February 6, 1992; Revised Manuscript Received July 16, 1992

ABSTRACT: Using site-specific mutagenesis, we have constructed two mutants of *Escherichia coli* dihydrofolate reductase (ecDHFR) to investigate further the function of a weakly acidic side chain at position 27 in substrate protonation: Asp27 → Glu (D27E) and Asp27 → Cys (D27C). The crystal structure of D27E ecDHFR in a binary complex with methotrexate shows that the side-chain oxygen atoms of Glu27 are in almost precisely the same location as those of Asp27 in the wild-type enzyme. Kinetic evidence indicates that Glu27 can indeed function efficiently in the proton relay to dihydrofolate. Even though vertebrate DHFRs all have a glutamic acid at the structurally equivalent position, the kinetic properties of Glu27 ecDHFR more closely resemble those of wild-type bacterial DHFRs than of vertebrate DHFRs. The D27C mutation produced an enzyme still capable of relaying a proton to dihydrofolate, but with the intrinsic pK_a in its pH–activity profiles shifted upward to values characteristic of the more basic thiolate group. The crystal structure of the binary complex with methotrexate reveals two unexpected features: (1) the Cys27 sulfhydryl group does not point toward the pteridine-binding site, but the side chain of this residue is instead rotated 120° to interact with a tyrosine side chain projecting from a neighboring β-strand; (2) a bound ethanol molecule occupies a cavity adjacent to methotrexate. Ethanol is a component of the crystallization medium.

Dihydrofolate reductase (DHFR;[1] EC 1.5.1.3) catalyzes the reduction of dihydrofolate (DHF) (and to a limited extent, folate) to tetrahydrofolate (THF). DHFR has been the subject of numerous studies aimed at understanding every aspect of its structure and function [for reviews, see Blakely (1984) and Kraut and Matthews (1987)]. We have chosen an approach utilizing site-specific mutagenesis coupled with X-ray crystallography and kinetic characterization to investigate wild-type (wt) and mutant *Escherichia coli* DHFRs (ecDHFRs).

Reduction of the N5=C6 double bond in DHF to form THF involves transfer of a hydride ion to C6 and a proton to N5. The source of the hydride ion is the cofactor NADPH, and the absolute stereochemistry of the hydride-transfer reaction has been determined to involve the *si* face of DHF and the cofactor's dihydronicotinamide ring 4-*pro-R* hydrogen (Charlton et al., 1979). All known chromosomally encoded DHFR sequences include a carboxylic acid side chain residing in the pteridine-binding site (Matthews et al., 1977, 1978; Baker et al., 1981; Volz et al., 1982; Stammers et al., 1987; Oefner et al., 1988), and previous mutagenesis studies have implicated this side chain in proton donation to N5 (Howell et al., 1986). In particular, this sequence position, Asp27 in ecDHFR, was mutated to asparagine (D27N) (Villafranca et al., 1983), and a primary site reversion of D27N to serine (D27S) was also characterized (Howell et al., 1986). These mutations resulted in functional albeit crippled enzymes with catalytic activity comparable to the wt only at low pH. In this study, we further investigate the mechanistic role of a prototropic group at position 27 by replacement of Asp27 with glutamic acid (D27E), which is nearly identical in function to aspartic acid, and by cysteine (D27C), which is almost isosteric with serine.

In the vertebrate DHFRs, Asp27 is replaced by glutamic acid, which has one more methylene unit in its side chain. Vertebrate DHFRs differ kinetically from bacterial DHFRs in several ways. Human DHFR does not exhibit apparent pK_a values in its steady-state pH–activity profiles with respect to the rate of DHF reduction (Beard et al., 1989; Schweitzer et al., 1989). In contrast, bacterial DHFR pH–activity profiles do exhibit kinetic pK values that are about 3 pK units higher than the pK_a of free aspartic acid (Stone & Morrison, 1984; Andrews et al., 1989). A second significant kinetic distinction is that while folate is a poor substrate for *E. coli* DHFR, it is turned over at an appreciable rate by vertebrate DHFRs. Finally, differences in their trimethoprim (TMP)-binding affinities between vertebrate and bacterial DHFRs are so great that TMP is used clinically as an antibacterial agent. Although it would be naive to assume that such differences between evolutionary distant species of DHFR could be due to a single amino acid change, we were nevertheless interested to see how such a seemingly small perturbation as aspartic acid to

[†] Supported by NIH Grants CA17374 and GM10928 to J.K. and GM35308 to E.E.H.

[‡] Refined coordinates for both mutant structures have been deposited to the Brookhaven Protein Data Bank under identification codes 1DRA and 1DRB.

* Author to whom correspondence should be addressed.

[§] University of California, San Diego.

[∥] University of Tennessee.

[⊥] Agouron Pharmaceuticals, Inc.

[#] Deceased 1988.

[1] Abbreviations: *E. coli*, *Escherichia coli*; *L. casei*, *Lactobacillus casei*; DHFR, dihydrofolate reductase; ecDHFR, *E. coli* DHFR; mDHFR, mouse DHFR; DHF, dihydrofolate; THF, tetrahydrofolate; NADP(+/H), nicotinamide adenine dinucleotide phosphate (oxidized/reduced); MTX, methotrexate; TMP, trimethoprim; wt, wild type; D27S, Asp27 → Ser mutant ecDHFR; D27E, Asp27 → Glu mutant ecDHFR; D27C, Asp27 → Cys mutant ecDHFR; D27N, Asp27 → Asn mutant ecDHFR; D27L, Asp27 → Leu mutant ecDHFR.

0006-2960/92/0431-9813$03.00/0

glutamic acid would affect the enzyme-catalyzed reaction rates for both DHF and folate and, in particular, whether the substitution might create an enzyme with catalytic and inhibitor-binding properties more nearly resembling those of the vertebrate DHFRs. Also of interest from a purely structural point of view was how the increased side-chain length of glutamic acid would be accommodated. A refined high-resolution crystal structure of wt ecDHFR·MTX (Bolin et al., 1982; Filman et al., 1982) is available for comparison.

Replacement of Ser27 in D27S ecDHFR by cysteine is also a seemingly minimal perturbation. The atomic radius of sulfur is 1.04 Å, as compared with oxygen's 0.66 Å. Bond lengths at the cysteine sulfur are longer than those at the hydroxyl oxygen in serine by about 0.4 Å, while the Cβ–Sγ–H angle is less by 14° than the corresponding angle in serine (Kistenmacher et al., 1974; Kerr et al., 1975). As mentioned above, the D27S mutation caused greatly diminished enzymic activity relative to wt at neutral pH and above owing to the inability of the mutant enzyme to protonate bound substrate. We were curious to see whether a thiol group replacing the hydroxyl of serine-27 could participate in substrate protonation because of its lower pK_a and thereby enhance the D27C enzyme's high-pH activity relative to D27S.

MATERIALS AND METHODS

Materials. Ampicillin, TMP, kanamycin, MTX, NADPH, and folate were purchased from Sigma Chemical Co. DHF was prepared by reduction of folate with sodium dithionite according to the procedure of Blakely (1960). It was stored at −20 °C in 5 mM HCl and 50 mM β-mercaptoethanol until used. Tetrahydrofolate was prepared and purified as described by Mathews and Huennekens (1960). NADPD used to measure primary kinetic isotope effects was prepared by the method of Viola et al. (1979) and Hermes et al. (1984) and purified by column chromatography (Viola et al., 1979; Vanoni & Matthews, 1984).

Mutagenesis. Mutant ecDHFRs were constructed by site-specific mutagenesis as previously described (Villafranca et al., 1983). pUC8 plasmids containing the mutated *fol* genes were transformed into a Fol$^-$ (null allele) strain of *E. coli* (Howell et al., 1988) to eliminate any background enzymic activity due to chromosomally encoded wt ecDHFR. Twelve liters of TB media (Tartof & Hobbs, 1987), inoculated with a culture grown overnight from cells stored at −70 °C, was incubated with shaking at 30 °C for approximately 26 h. The large culture contained 200 μg/mL ampicillin and 25 μg/mL kanamycin. In addition to the aforementioned antibiotics, the starter culture also included 20 μg/mL TMP. Cells from the starter culture were washed twice with plain medium before they were used to infect the large volume of broth. Purification of the mutant proteins was essentially as described by Villafranca et al. (1983). Preparations were judged to be pure by the presence of a single band on SDS–PAGE gels stained with Coomassie blue. A typical yield was 15 mg of protein/L of medium.

Cysteine Content of D27C Mutant. The number of cysteine residues in D27C ecDHFR was quantified by the method of Ellman (1959).

Kinetic Characterization. Measurements of steady-state kinetic parameters, k_{cat} and $K_{m(DHF)}$, were performed under the same conditions as reported previously (Howell et al., 1987). Correction for a background rate due to the decomposition of substrate and cofactor was made either by including all components of the reaction mixture, except the enzyme, in the reference cuvette or by determining the rate in the absence of enzyme and subtracting this base-line rate from the measured rate. Prior to inclusion in the assay mixture, enzymes were preincubated with a saturating concentration of NADPH to avoid hysteretic effects (Penner & Frieden, 1985). Initial rate data were fitted directly to the Michaelis–Menten equation using the computer programs Enzfitter and/or GraFit (Elsevier-BIOSOFT) which employ nonlinear regression methods to calculate V_{max} and K_m. Apparent pK_a values from pH profiles [log k_{cat} vs pH or log ($k_{cat}/K_{m(DHF)}$) vs pH] were calculated for the D27E and D27C mutant ecDHFRs using an equation that compensates for slopes differing from unity (Murphy & Benkovic, 1989).

Pre-steady-state measurements were conducted on a HI-TECH SF51 stopped-flow spectrophotometer at 20 °C. Rate constants for hydride transfer for wt and D27E ecDHFRs were generated from best fits of stopped-flow traces to the kinetic scheme of wt ecDHFR (Fierke et al., 1987) using the computer program KINSIM (Barshop et al., 1983). KINSIM simulates reaction time courses by numerically integrating the rate equations corresponding to an entire kinetic scheme. Both the pre-steady-state burst and the linear steady-state phases of enzyme turnovers were fitted simultaneously. Simulated stopped-flow traces were calculated using scaling factors that contained terms for contributions to the total fluorescence signal from the ternary cofactor–substrate complexes, binary cofactor complexes, and free ligands. In the case of D27C ecDHFR, no pre-steady-state burst of product formation occurs. The rate of hydride transfer for this mutant was estimated from fits of absorbance transients (340 nm) for single enzyme turnovers at less than stoichiometric concentrations of NADPH. Association and dissociation rate constants for coenzyme were obtained by stopped-flow fluorescence quenching (Dunn & King, 1980; Cayley et al., 1981). Dissociation rates for DHF and THF were measured by competition methods (Fierke et al., 1987) using TMP or MTX as trapping ligands; $NADP^+$ was used to trap free enzyme when monitoring NADPH dissociation. All solutions were buffered with either 50 mM Tris [tris(hydroxymethyl)aminomethane], 25 mM Mes [2-(*N*-morpholino)ethanesulfonic acid], 25 mM acetic acid, and 0.1 M NaCl or 33 mM succinic acid, 44 mM imidazole, 44 mM diethanolamine, and 0.1 M NaCl.

The ability of the mutant enzymes to reduce folate was checked by a modified version of the technique of Kaufman and Gardiner (1966). A 10-μL aliquot of folate (10–100 μM final concentration) was added to 700 μL of buffer (125 mM potassium acetate, pH 4.75 or pH 5.25, or 125 mM sodium acetate, pH 6.00), mixed by inversion, followed by the addition of 20 μL of an enzyme·NADPH mixture. The final NADPH concentration was 100 μM. Final enzyme concentrations ranged from 56.0 nM to 6.00 μM. After mixing by inversion, the cuvette containing the assay mixture was placed in a Perkin-Elmer Lambda 3B spectrophotometer, and the rate of the reaction was followed by monitoring the decrease in absorbance at 340 nm for 60 s at 30 °C. Data points were collected by a Zenith Z-150 PC connected to the spectrophotometer. A base-line rate due to the decomposition of cofactor and substrate was determined in the absence of enzyme and subtracted from the measured rates. Absorbance versus time plots were analyzed using the UVS software programs developed by Gene Gould at Softways, Moreno Valley, CA.

K_d of MTX. Thermodynamic dissociation constants for MTX [$K_{d(MTX)}$] were determined at 4 °C by equilibrium dialysis using the procedure of Howell et al. (1987).

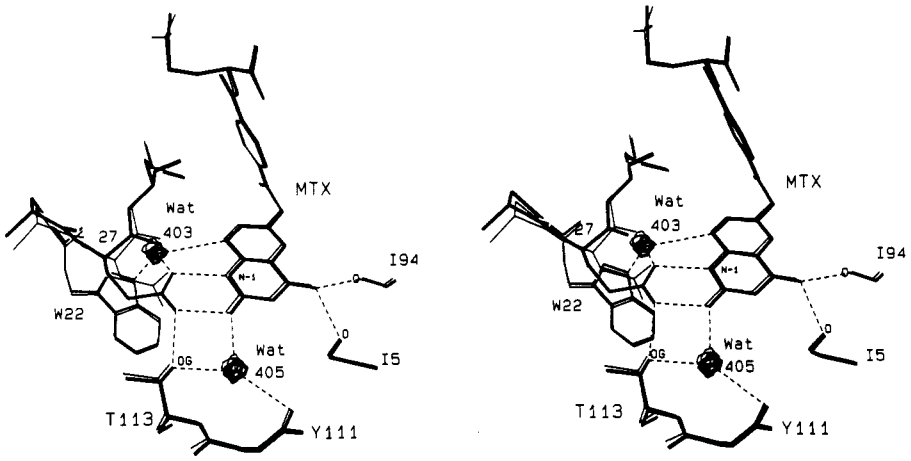

FIGURE 1: Comparison of pteridine-binding sites in wild-type ecDHFR and D27E mutant ecDHFR in binary complexes with methotrexate (MTX). Molecule 1 of the asymmetric unit is shown. The heavy line is D27E ecDHFR; the thin line is wild-type ecDHFR. Water molecules (Wat) are represented by spheres. Dashed lines indicate hydrogen bonds. Refined coordinates were superpositioned using the program OVRLAP (Rossman & Argos, 1975). The distance between Glu27 Oε1 of D27E and Asp27 Oδ1 of wild-type ecDHFR is 0.60 Å. The largest distance between identical MTX atoms in the two structures is 0.3 Å between the 2-amino nitrogens.

MTX-Binding UV Difference Spectra. Ultraviolet difference spectra were examined in order to ascertain the protonation state of MTX in binary complexes with the mutant enzymes. MTX-binding UV difference spectra were generated by subtracting the spectrum of unmixed solutions of enzyme and MTX at neutral pH from the spectrum obtained when the two solutions were mixed. The experimental conditions were the same as in Howell et al. (1986).

Crystallography. Crystals of the mutant enzymes in binary complex with MTX were grown in sitting drops at 4 °C by vapor diffusion. A solution of 30 mg/mL ecDHFR containing a 2-fold molar excess of MTX over DHFR in Tris-HCl, pH 7.3, was mixed with histidine hydrochloride, pH 6.8, and calcium acetate. Final concentrations were 80 mM Tris-HCl, 50 mM histidine hydrochloride, and 1.0 mM calcium acetate. The reservoir contained 15% ethanol in 0.10 M Tris-HCl, pH 7.3. X-ray diffraction data were collected to 1.9 Å on each mutant using a Xuong-Hamlin multiwire area detector diffractometer (Xuong et al., 1978); each data set contained reflections from a single crystal. Initial electron density difference maps of the mutants minus wt were calculated using coefficients $(F_{mut} - F_{wt})e^{i\alpha}$, where F_{wt} and F_{mut} are the observed wt and mutant structure factor amplitudes and α represents phases from the earlier refinement of the cloned wt structure (Howell et al., 1986). Maps were viewed and interpreted on a Silicon Graphics IRIS picture system running FRODO (Jones, 1978) and MMS (Dempsey, 1987). Models of the mutant DHFRs were constructed by replacement of aspartic acid-27 with either cysteine or glutamic acid. Each model was refined to convergence[2] using the program PROLSQ (Hendrickson & Konnert, 1980).

RESULTS AND DISCUSSION

Crystal Structure Statistics

Mutant protein crystals were isomorphous with wt ecDHFR·MTX (Matthews et al., 1977); space group $P6_1$, two molecules per asymmetric unit. Unit-cell parameters differed by less than 0.5% from the wt. After least-squares refinement, final R-factors and root-mean-square deviations from ideal bond lengths were 15.3% and 0.013 Å, respectively, for D27E ecDHFR·MTX and 14.9% and 0.017 Å, respectively, for D27C ecDHFR·MTX, where $R = \Sigma|F_o - F_c|/\Sigma F_o$ and F_o and F_c are the observed and calculated structure factor amplitudes, respectively. Convergence was reached after 18 refinement cycles for the D27E ecDHFR structure and after 28 cycles for D27C ecDHFR. The average error in the atomic positions was estimated to be 0.15 Å by the method of Luzzati (1952).

D27E ecDHFR

Description of D27E ecDHFR·MTX Crystal Structure. The refined crystal structure of the binary D27E ecDHFR·MTX complex is virtually identical to the wt ecDHFR·MTX structure solved previously (Matthews et al., 1977; Bolin et al., 1982). No major structural changes are seen in the region around sequence position 27. The carboxyl oxygen atoms of the Glu27 side chain are in almost the same location as those of Asp27 in wt ecDHFR. Viewed from above the pteridine-binding site, the additional methylene group of glutamic acid is accommodated by a kinking of the side chain below the pteridine plane (see Figure 1). Glu27 side-chain torsion angles are comparable to those seen in the analogous Glu30 residue in the chicken liver DHFR·biopterin·NADP$^+$ (M. McTigue, personal communication) and recombinant human DHFR·folate (Davies et al., 1990) crystal structures. The hydrogen-bonding pattern linking the surrounding side chains and bound waters is the same in this mutant as in the wt ecDHFR·MTX structure. Glu27 Oε1 is hydrogen-bonded to Thr113 Oγ1 and the 2-amino group of MTX. The other carboxyl oxygen, Oε2, is hydrogen-bonded to water 403/603[3] and MTX N1. Water 403/603 is within hydrogen-bonding distance of Trp22 Nε1 and N8 of MTX. Water 405/639, hydrogen-bonded to Thr113 Oγ1, the MTX 2-amino group,

[2] The refined coordinates of D27E and D27C ecDHFR have been deposited in the Protein Data Bank at Brookhaven National Laboratory.

[3] The numbering system for bound water molecules varies from one crystal structure to another. In the *E. coli* DHFR binary complex with MTX, each water has two numbers associated with it because there are two protein molecules in the asymmetric unit. The *E. coli* DHFR·folate binary and *E. coli* DHFR·folate·NADP$^+$ ternary structures have one molecule in the asymmetric unit; hence, each water molecule has only one number. Equivalences of active-site waters in *E. coli* DHFR crystal structures are as follows: water 403/603 in ecDHFR·MTX is the same as water 206 in the folate binary and ternary complexes; water 405/639 in ecDHFR·MTX is the same as water 301 in the folate binary and ternary complexes.

Table I: Steady-State Kinetic Parameters at pH 7.0

DHFR	k_{cat} (s^{-1})	$K_{m(DHF)}$ (μM)	$k_{cat}/K_{m(DHF)}$ (s^{-1} M^{-1})
wild type[a]	30 ± 1.0	1.2 ± 0.19	(2.5 ± 0.44) × 10^7
D27S[b]	0.41 ± 0.0082	56 ± 2.4	(7.3 ± 0.34) × 10^3
D27E	41 ± 1.5	27 ± 3.2	(1.5 ± 0.18) × 10^6
D27C	2.2 ± 0.16	130 ± 15	(1.7 ± 0.23) × 10^4

[a] Howell et al. (1986). [b] Howell et al. (1990).

and the backbone carbonyl oxygen of Tyr111, is also preserved in the D27E ecDHFR·MTX crystal structure.

The inhibitor MTX occupies the same position as in the wt structure, with its 4-amino group hydrogen-bonded to the backbone carbonyl oxygens of Ile5 and Ile94. However, in molecule 1 of the asymmetric unit, but not molecule 2, the γ-carboxylate oxygens of the glutamyl portion of the inhibitor are not quite coincident with those of the MTX in wt ecDHFR·MTX, but are displaced by a 29° rotation about Cγ–Cδ. These oxygen atoms exhibit high individual temperature factors in both the wt ecDHFR·MTX structure (Bolin et al., 1982) and the mutant, indicating that their positions are not well-defined.

To further characterize MTX binding to D27E, we investigated the protonation state of enzyme-bound MTX and measured the dissociation constant of MTX from the D27E ecDHFR·MTX binary complex.

Protonation of MTX Bound to D27E ecDHFR. Other workers have used ultraviolet (UV) difference spectroscopy to investigate the protonation state of ligands bound to DHFRs from various species, both eucaryotic (Poe et al., 1975) and procaryotic (Erickson & Mathews, 1972; Poe et al., 1974; Hood & Roberts, 1978). The MTX-binding UV difference spectrum obtained with wt ecDHFR shows the same features as the difference spectrum of neutral versus protonated MTX in solution, indicating that MTX is protonated at N1 in the binary complex with wt ecDHFR at neutral pH. In contrast, both the D27N and D27S mutants have MTX-binding UV difference spectra that do not match that of wt ecDHFR, suggesting that these mutations disrupt the ability of ecDHFR to protonate bound MTX (Howell et al., 1986). Additional evidence confirming that MTX is protonated when bound to wt but unprotonated when bound to D27S was obtained from ^{13}C NMR studies (London et al., 1986). For the D27E mutant, the MTX-binding UV difference spectrum closely resembles that obtained with the wt enzyme, indicating that D27E can also protonate bound MTX (data not shown). Altogether we have studied MTX-binding UV difference spectra for four mutants at this site: D27N, D27S, D27E, and D27C; only D27E gives a result similar to that obtained with wt ecDHFR. Previously solved crystal structures showed that the wt enzyme's Asp27 side chain makes an ionic interaction with N1 of MTX (Matthews et al., 1977; Bolin et al., 1982). In the case of the present D27E structure, protonation of bound MTX is consistent with the crystallographically observed preservation of that interaction.

K_d of MTX. The dissociation constant, $K_{d(MTX)}$, was determined to be 12 ± 1.2 nM for D27E ecDHFR·MTX. Wt ecDHFR exhibits a much tighter binding of MTX; the previously measured dissociation constant for wt is 0.068 ± 0.0043 nM (Howell et al., 1986).

Enzymic Activity of D27E ecDHFR toward DHF. The steady-state kinetic parameters k_{cat}, $K_{m(DHF)}$, and $k_{cat}/K_{m(DHF)}$ at pH 7.0 for wt and D27E ecDHFR are given in Table I. At neutral pH, the activity of D27E, as measured by k_{cat}, is 1.4 times greater than wt, but since the mutant's $K_{m(DHF)}$ is increased by 23-fold, the apparent second-order rate constant, $k_{cat}/K_{m(DHF)}$, is 17 times less than wt.

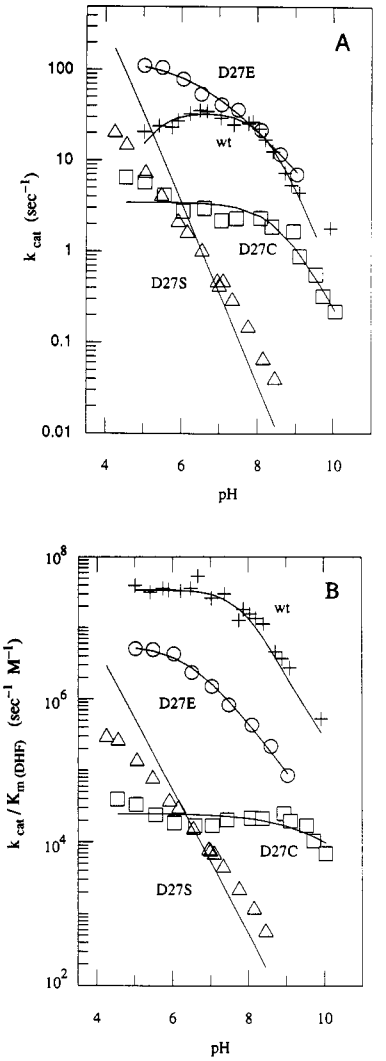

FIGURE 2: pH–activity profiles under steady-state conditions. (A) log k_{cat} vs pH; (B) log [$k_{cat}/K_{m(DHF)}$] vs pH. (+) Wild-type ecDHFR; (△) D27S ecDHFR; (○) D27E ecDHFR; □ D27C ecDHFR. NADPH was held at a saturating concentration, generally 100 μM. The buffer was 33.0 mM succinic acid, 44.0 mM imidazole, 44.0 mM diethanolamine, and 10.0 mM β-mercaptoethanol. The temperature was 30 °C. Enzyme concentration ranges were as follows: wild-type ecDHFR, 0.69–6.2 nM; D27S ecDHFR, 19–1900 nM; D27E ecDHFR, 0.67–14 nM; D27C ecDHFR, 27–350 nM. Experimental data were fitted to the following equations: wild-type ecDHFR, eq 5 of Stone and Morrison (1984); D27S ecDHFR, eq 1 and 2 in Howell et al. (1986); D27E and D27C ecDHFR, equation given by Murphy and Benkovic (1989).

The pH dependence of the steady-state kinetic parameters, k_{cat} and $k_{cat}/K_{m(DHF)}$, for D27E is shown in Figure 2. Also shown are the curves for wt, D27S (Howell et al., 1986), and D27C (see below for discussion of this mutant). As for wt, the D27E activity vs pH curves exhibit apparent pK_a's within the accessible pH range. The apparent pK_a values are as follows: k_{cat}, 6.5 ± 0.1; $k_{cat}/K_{m(DHF)}$, 6.5 ± 0.1. Although the k_{cat} for D27E is greater than for wt at pH values less than 7.5, the K_m has increased across the accessible pH range, resulting in lower values for $k_{cat}/K_{m(DHF)}$ at every pH.

Insight into the kinetic behavior of DHFR can be gained from pre-steady-state hydride-transfer and ligand-binding rate measurements. As shown in Table II, the hydride-transfer rate constant, $k_{hydride}$, for D27E is 1.7 times lower at pH 5.0 and 3.4 times lower at pH 7.3 than the wt rate constant.

Table II: Pre-Steady-State Ligand-Binding and Hydride-Transfer Rate Constants

rate	units	pH	wt	D27E	D27C
$k_{on(NADPH)}$	$s^{-1}\ \mu M^{-1}$	8.0	18 ± 1.0	15 ± 1.2	13 ± 1.5
$k_{off(NADPH)}$	s^{-1}	8.0	10 ± 4	22 ± 1	30 ± 3
$k_{off(DHF)}$	s^{-1}	5.5	19 ± 0.2	305 ± 20	
$k_{off(THF)}$	s^{-1}	6.0	1.0 ± 0.15	29.6 ± 2.0	
$k_{hydride}$	s^{-1}	5.0	770 ± 90	460 ± 35	
		7.3	135 ± 15	40 ± 6	1.7 ± 0.2

Table III: Primary Deuterium Isotope Effects

DHFR	pH	^{D}V	$^{D}[V/K_{m(DHF)}]$
wild type	5.1[a]	1.2	1.1
	6.0[b]	1.0	nd[c]
	9.0[b]	2.7	3.0
D27S[a]	5.1	3.2	3.6
	7.0	3.3	3.1
	9.0	3.2	3.3
D27E	5.0	1.4	1.6
	7.0	1.8	3.3
	9.0	2.8	3.6
D27C	5.0	2.5	2.8
	7.0	2.7	3.3
	9.0	2.9	3.3

[a] Howell et al. (1987). [b] Chen et al. (1987). [c] nd = not determined.

Nevertheless, hydride transfer evidently is still not entirely rate-limiting at low pH since the mutant enzyme fails to exhibit a full isotope effect in ^{D}V [that is, in $k_{cat(NADPH)}/k_{cat(NADPD)}$] until the pH is greater than 7 (see Table III). At pH 9, ^{D}V approaches 3 for both D27E and wt, indicating that hydride transfer becomes more nearly rate-limiting at high pH.

As shown in Table II, the on–off rate constants, $k_{on(NADPH)}$ and $k_{off(NADPH)}$, for the binary complex D27E·NADPH are similar to those for wt ecDHFR. The association rate constants are essentially equal, and the dissociation rate constants are within a factor of 2. These results indicate that the mutation has not significantly affected cofactor binding in the binary complex.

In contrast, the binding kinetics of both DHF and THF are substantially altered in the D27E mutant. At pH 6.0, the THF dissociation rate constant, $k_{off(THF)}$, is 30 times greater for this mutant than for the wt. Similarly, the DHF dissociation rate constant, $k_{off(DHF)}$, is elevated 14-fold as compared with wt. Fierke et al. (1987) have shown that the rate-limiting step for wt ecDHFR at low pH is dissociation of THF from the mixed product–reactant complex DHFR·THF·NADPH. Based on the increased values for $K_{m(DHF)}$, $k_{off(DHF)}$, and $k_{off(THF)}$ of D27E, a reasonable explanation for its elevated values of k_{cat} at low pH is that the mutant has an increased THF dissociation rate from the enzyme·THF·NADPH complex.

The apparent pK_a of 6.5 seen in the log k_{cat} vs pH profile for D27E matches the intrinsic pK_a of Asp27 in the wt ternary complex, DHFR·DHF·NADPH, obtained by examining the pH dependence of hydride-transfer rates using stopped-flow techniques (Fierke et al., 1987). However, since the D27E mutant's hydride-transfer rate is not solely rate-limiting at low pH, the intrinsic pK_a of Glu27 is probably somewhat lower than 6.5. In fact, the pH dependence of hydride transfer for D27E yields a pK_a of 6.2 ± 0.1 (data not known). In the case of the wt enzyme, the perturbation is much larger, with an apparent pK_a of 8.4 in its log k_{cat} vs pH profile (Stone & Morrison, 1984) as compared with an intrinsic pK_a of 6.5. This shift has been shown to be due to a change in the rate-limiting step from THF dissociation to hydride transfer as the pH is increased (Fierke et al., 1987). For D27E, the smaller shift from 6.2 to 6.5 is probably a consequence of the observed decreased rate of hydride transfer and the inferred increased rate of THF dissociation.

Pteridine Ligand Binding to D27E ecDHFR. Insertion of an additional methylene group into the side chain of Asp27 by mutation to Glu27 results in an enzyme molecule that is structurally almost identical to the wt, but one with altered kinetic and binding properties. Although the crystal structure indicates that Glu27 is hydrogen-bonded to MTX and the MTX-binding difference spectrum obtained with D27E suggests that bound MTX is protonated, the binary complex dissociation constant for MTX is elevated relative to wt by almost 200-fold.

The increased $K_{d(MTX)}$ of D27E may be a consequence of a decreased MTX k_{on} rate and/or an increase in the rate of k_{off} of MTX. The latter seems likely in view of the observed increases in $k_{off(DHF)}$ and $k_{off(THF)}$ for the mutant. Evidence bearing on the former comes from the crystal structures of *E. coli* and chicken liver DHFR indicating that a glutamic acid side chain in this position may be more flexible than an aspartic acid side chain. In the chicken liver DHFR·NADPH structure, electron density corresponding to Glu30 is weak beyond the Cγ atom (Kraut & Matthews, 1987), but electron density for this side chain is well-defined in complexes that have a phenyltriazine [2,4-diamino-5,6-dihydro-6,6-dimethyl-5-(4-methoxyphenyl)-*s*-triazine] (Volz et al., 1982) or TMP (Matthews et al., 1985) in the pteridine-binding site. Both TMP and the phenyltriazine interact with Glu30 via hydrogen bonds and salt bridges that are identical to the interactions found between Asp27 and MTX in the wt ecDHFR·MTX structure. In contrast, the electron density for the entire side chain of Asp27 is well-defined even in the ecDHFR apoenzyme and holoenzyme crystal structures (Bystroff et al., 1990) when the pteridine-binding site is unoccupied. If D27E does have a decreased $k_{on(MTX)}$, this could be a reflection of the requirement that a partially disordered Glu27 side chain must be ordered to make favorable interactions with MTX. Perhaps the same phenomenon also accounts for the elevated $K_{m(DHF)}$ and increased DHF and THF dissociation rates displayed by the mutant (see Table II).

Enzymic Activity of D27E ecDHFR toward Folate. DHFRs from vertebrate sources reduce folate at higher rates than does ecDHFR (Nakamura & Littlefield, 1972; Morandi & Attardi, 1981; Selinsky et al., 1990; Thillet et al., 1990; Howell et al., 1990). For example, at pH 5 k_{cat} for folate reduction by mouse DHFR (mDHFR) is approximately 400 times greater than the ecDHFR rate constant (Thillet et al., 1990; Howell et al., 1990). Amino acid sequence comparisons show that ecDHFR has aspartic acid at position 27 while vertebrate DHFRs have glutamic acid at the equivalent position (Freisheim & Matthews, 1984). To see if the side-chain length might be related to the difference in specificity toward folate, we examined the rate of folate reduction by D27E ecDHFR. Reduction of folate by the mutant enzyme was found to be immeasurably slow, even at the highest enzyme concentrations. In fact, at pH 6.0 and 7.0, the rate of absorbance change was actually less than the background rate, suggesting that D27E ecDHFR was probably binding and protecting folate and/or NADPH from nonenzymic breakdown. At low pH, the rate of absorbance change was slightly greater than the background rate, but when the background rate was subtracted, the data could still not be fitted to the Michaelis–Menten equation. In contrast, both

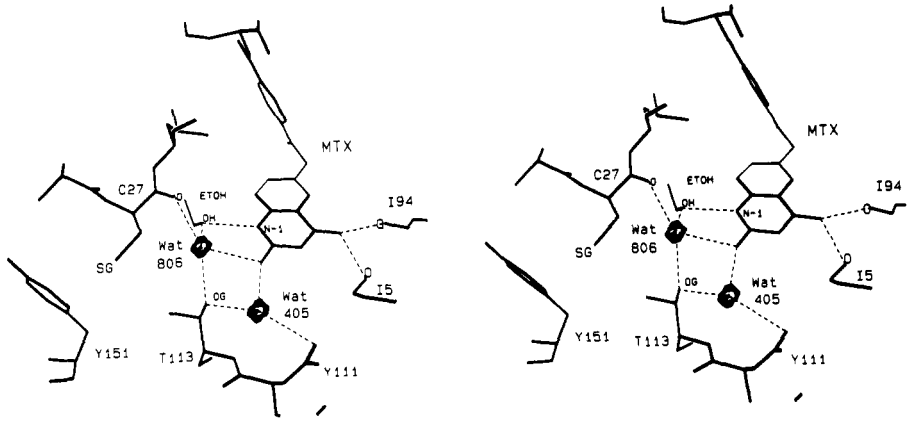

FIGURE 3: 1.9-Å X-ray structure of the D27C ecDHFR pteridine-binding site in binary complex with methotrexate (MTX). Molecule 1 of the asymmetric unit is shown. Probable hydrogen bonds are shown by dashed lines. Spheres depict water (Wat) molecules.

wt ecDHFR and recombinant human DHFR reduce folate quite readily under the same conditions, yielding steady-state kinetic parameters k_{cat} and $K_{m(folate)}$ within experimental error of their published values (Howell et al., 1990; Morandi & Attardi, 1981).

While substitution of glutamic acid for Asp27 at the structurally equivalent position may or may not be important for the enhanced rate of folate reduction by vertebrate DHFRs, the same substitution in ecDHFR fails to make that mutant enzyme resemble its vertebrate counterparts in that regard. D27E's lack of activity toward folate may be due to a low turnover rate and/or loose binding, as noted previously for DHF reduction. A different conclusion, however, was drawn by Thillet et al. (1990), who recently reported that an E30D mutant of mDHFR has a diminished capacity to reduce folate compared to the wt mDHFR. The k_{cat}, at pH 6, for wt mDHFR is 0.44 s^{-1}; for E30D mDHFR, it is 0.060 s^{-1}. Because the k_{cat} for E30D mDHFR is similar to the k_{cat} measured for *Lactobacillus casei* DHFR (0.066 s^{-1}; Andrews et al., 1989), they argued that this residue is responsible for the difference in the rates of folate reduction between bacterial and vertebrate DHFRs (*L. casei* DHFR also has aspartic acid at the position corresponding to Asp27 in ecDHFR). However, in order to properly compare substrate specificities, the kinetic parameter $k_{cat}/K_{m(folate)}$ for each enzyme should be examined. Such a comparison between three vertebrate DHFRs (cow, mouse, and the mouse E30D mutant) and two bacterial DHFRs (*L. casei* and *E. coli*) reveals that the *L. casei* enzyme is more like the DHFR from vertebrates and that the ability of E30D mDHFR to catalyze the reduction of folate actually does not vary significantly from the wt mDHFR. Values for $k_{cat}/K_{m(folate)}$ in units of s^{-1} M^{-1} are the following: cow DHFR, 3.5×10^4, pH 6 (Selinsky et al., 1990); mDHFR, 4.4×10^4, pH 6 (Thillet et al., 1990); E30D mutant mDHFR, 2.0×10^4, pH 6 (Thillet et al., 1990); *L. casei* DHFR, 5×10^4, pH-independent rate (Andrews et al., 1989); and ecDHFR, 4.5×10^2, pH 5 (Howell et al., 1990). It might be mentioned, as an aside, that there may be an evolutionary reason why *L. casei* DHFR is better at reducing folate than are other bacterial DHFRs. Since *L. casei* cannot synthesize DHF (Kisliuk, 1984), this bacterium, like the animals, has a nutritional requirement for folates which can be fulfilled by the fully oxidized form of the compound. Indeed, *L. casei* has an active transport system for the uptake of folates (Huennekens & Henderson, 1975) that makes it useful in folate assays (Cossins, 1984).

Further Comparisons between D27E ecDHFR and Vertebrate DHFRs. In addition to its inability to efficiently reduce folate, other kinetic properties of the D27E mutant also more closely resemble those of wt ecDHFR than of vertebrate DHFRs. Profiles of steady-state kinetic parameters vs pH for D27E are similar to pH profiles for wt ecDHFR but unlike pH profiles for human DHFR. Both wt ecDHFR and D27E exhibit distinct apparent pK values in their pH–activity profiles while human DHFR does not (Beard et al., 1989; Schweitzer et al., 1989). Also, D27E is more like wt ecDHFR than human DHFR with respect to its TMP affinity. Preliminary experiments indicate that the TMP inhibition constant, K_i, for D27E ecDHFR is 25 nM, which is closer to the wt ecDHFR K_i of 1.3 nM (Baccanari et al., 1982) than to the much larger value for human DHFR, 1.00 μM (Prendergast et al., 1989; David, 1992).

D27C ecDHFR

Cysteine Content of D27C. Wt ecDHFR contains two cysteine residues, at positions 85 and 152, which are not involved in a disulfide bond. As expected, three free sulfhydryl groups were found in the D27C mutant.

Discovery of Bound Ethanol Molecules in D27C and D27S ecDHFR·MTX Crystal Structures. In the wt ecDHFR·folate binary and wt ecDHFR·folate·$NADP^+$ ternary complex, water 206 is hydrogen-bonded to Oδ2 of Asp27, Nϵ1 of Trp22, and O4 of folate (Bystroff et al., 1990). Similarly, in the wt ecDHFR·MTX structure, N8 of MTX is in essentially the same position as O4 of folate, and the equivalent water 403/603 is hydrogen-bonded to Oδ2 of Asp27, Nϵ1 of Trp22, and N8 of MTX (Bolin et al., 1982). During the course of least-squares refinement of the isomorphous D27C ecDHFR·MTX structure, however, we observed that the electron density associated with water 403/603 was too extensive to be explained by a single water molecule, but not long enough to accommodate two water molecules. Since the crystallization medium for the MTX binary complexes included 15% ethanol, we suspected that the anomalous density might be due to a bound ethanol molecule. Water 403/603 was therefore removed from the model, and an ethanol molecule was fitted into the density. The ethanol oxygen atom was positioned within hydrogen-bonding distance of both MTX N1 and a new water molecule, water 806/808, described below (see Figure 3). If the ethanol were to be placed in the alternative orientation, with its C2 group near water 806/808, no hydrogen bonds involving its oxygen atom can be formed. Refinement of the structure including the bound ethanol molecule was continued to convergence. Final $F_o - F_c$ difference Fourier maps showed no unexplained residual density in the vicinity of the ethanol molcules.

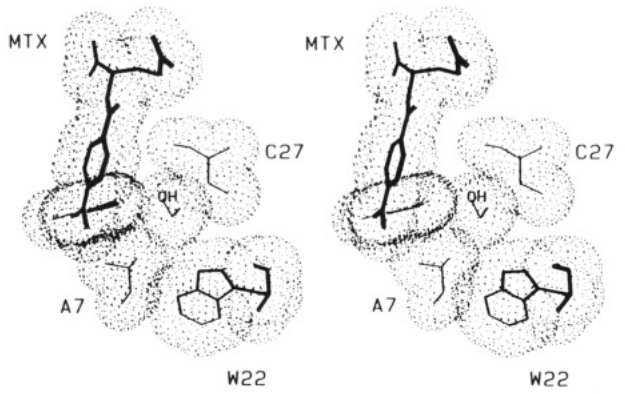

FIGURE 4: View of the D27C ecDHFR·MTX crystal structure emphasizing side-chain and inhibitor interactions with the bound ethanol molecule by showing van der Waals surfaces of methotrexate (MTX) and protein side chains surrounding the ethanol.

Since all of our mutant ecDHFR·MTX crystals had been grown with ethanol as precipitant, we reexamined the last D27S ecDHFR·MTX electron density map to see whether an ethanol molecule might be present in that structure as well. When an ethanol molecule was aligned with its oxygen atom superimposed on what had earlier been assumed to be water 885/805, its two carbon atoms could indeed be fitted into a feature previously described as elongated electron density in the direction of water 403/603 (Howell et al., 1986). Water 403/603 occurs in the wt ecDHFR·MTX structure but not in D27S ecDHFR·MTX or D27C ecDHFR·MTX.

We now believe that both D27S ecDHFR·MTX and D27C ecDHFR·MTX crystal structures contain bound ethanol molecules as described. Ethanol, present during crystallization, is able to bind at this site because it can donate a hydrogen bond to MTX N1 and accept a hydrogen bond from water 806/808 (or the serine hydroxyl in the case of D27S), as well as make favorable hydrophobic interactions with MTX and the side chains of Ala7 and Trp22 (see Figure 4). The other ecDHFR·MTX crystal structures (wt, D27N, and D27E) do not bind ethanol at this site because Oδ2, Nδ2, or Oε2 of their residue 27 occupies the same position as the oxygen atom of ethanol in D27S and D27C ecDHFR. The position of wt Asp27 Oδ1 is occupied by water 806/808 in D27C and by the serine Oγ in D27S. Furthermore, wt, D27N, and D27E all have a water molecule, water 403/603, hydrogen-bonded to the aforementioned side-chain atoms.

Description of D27C ecDHFR·MTX Crystal Structure. The overall backbone folding of the D27C mutant is identical to that of wt ecDHFR·MTX. Differences between wt and D27C ecDHFR are confined to the site of mutation as detailed below.

Essential features of the pteridine-binding site in D27C ecDHFR·MTX are shown in Figure 3. The ethanol OH group is close to the position occupied by the Oδ2 carboxyl oxygen of Asp27 in the wt structure, whereas the position occupied by the other carboxyl oxygen, Oδ1, of Asp27 in the wt structure is now taken by a new water molecule, water 806/808. Water 806/808 donates hydrogen bonds to the oxygen atom of the ethanol molecule and to the backbone carbonyl oxygen of residue 27. It accepts hydrogen bonds from the 2-amino group of MTX and Oγ1 of Thr113. The sulfhydryl group of Cys27 is not near the bound MTX; rather, it is bent back away from the pteridine-binding site and is in van der Waals contact with the phenyl ring of Tyr151 located on an adjacent β-strand, βH. Other nearby residues, Thr113, Trp22, Ile5, and Ile94, all maintain the same positions as in the wt ecDHFR·MTX structure. Similarly, water 405/639 is still hydrogen-bonded to Oγ1 of Thr113, to the backbone carbonyl oxygen of Tyr111, and to the 2-amino group of MTX. Completing the hydrogen-bonding network, N1 of MTX accepts a hydrogen bond from the ethanol hydroxyl group.

Interaction between Cys27 and Tyr151. The sulfur atom of Cys27 is pointed toward the phenyl ring of Tyr151 at an average distance of 3.9 Å from the ring carbon atoms. Levitt and Perutz have proposed that aromatic rings can act as hydrogen bond acceptors (Levitt & Perutz, 1988) when the bonded hydrogen atom is essentially pointed at the center of the ring. For the sulfhydryl hydrogen of Cys27 to interact with the ring centroid, the Cβ–S–H angle would have to be close to 150°. However, a neutron diffraction study of cysteine has determined this angle to be 96° (Kerr et al., 1975), which indicates that a direct hydrogen bond between the sulfhydryl hydrogen of Cys27 and Tyr151's phenyl ring is unlikely.

K_d and Protonation State of MTX Bound to D27C ecDHFR. The measured value for the MTX dissociation constant from a binary complex of D27C ecDHFR·MTX was 170 ± 33 nM. This $K_{d(MTX)}$ is 3-fold higher than that previously determined for D27S, 55 ± 7.0 nM (Howell et al., 1987). The MTX-binding UV difference spectrum of D27C did not correspond to the difference spectrum obtained with the wt enzyme (data not shown). Rather, it was similar to the MTX-binding difference spectra previously determined for D27S and D27N ecDHFR (Howell et al., 1986). This result indicates that, in agreement with expectation, the D27C mutant cannot protonate bound MTX.

Modeling the Pteridine-Binding Sites of D27C and D27S ecDHFR in the Absence of Bound Ethanol. Since ethanol was, of course, not a component of the kinetic assay or equilibrium dialysis buffers, in order to provide a sensible structural basis for interpreting kinetic and binding data on these mutants we must try to imagine what their pteridine-binding sites might look like in the absence of bound ethanol. To this end, the crystal structures of D27C and D27S were viewed with the aid of the program MMS, and after deletion of the ethanol molecules, minor modifications were made on the basis of hydrogen-bonding considerations and bearing in mind the similar values measured for $K_{d(MTX)}$ of D27C and D27S. We conclude from these modeling experiments that the originally published crystal structure of D27S ecDHFR·MTX was probably, after all, the correct model for the mutant enzyme molecule *in the absence of ethanol*. That is to say, the position of the ethanol's oxygen atom in the crystal structure probably is, after all, occupied by a bound water corresponding to water 885/805 since it could then form hydrogen bonds to both N1 of MTX and the Ser27 hydroxyl group. However, the side chain of Cys27 in the ethanol-free MTX complex of D27C probably has one more conformation available to it than does the side chain of Ser27 in the MTX complex of D27S, namely, a conformation in which it interacts with Tyr151. Upon inspection of the model, two distinct cases suggest themselves; in one, the Cys27 thiol group points into the pteridine-binding site, and in the other, it points away.

(*A*) *Case 1.* The χ^1 torsion angle of Cys27 was rotated from its D27C ecDHFR·MTX crystal structure conformation of 300° to an equally favorable $\chi^1 = 180°$ (McGregor et al., 1987). This rotation places the sulfhydryl group near Thr113 Oγ1 and across from MTX N1 (see Figure 3). Water 806/808 was removed along with the ethanol molecule, and another water was placed near the site formerly occupied by the oxygen atom of the ethanol, within hydrogen-bonding distance of MTX N8. The cysteinyl sulfur atom was within hydrogen-bonding

distance of this modeled water molecule. Although sulfur is usually thought of as a hydrogen bond acceptor in proteins (Adman et al., 1975; Katti et al., 1990), there is evidence from both small-molecule crystallography and recent protein structures that it can also function as a hydrogen bond donor (Srinivasan & Chacko, 1967; Kerr et al., 1975; Dreusicke et al., 1988; McGrath et al., 1989; Gregoret et al., 1991). Since it probably accepts a hydrogen bond from Thr113 Oγ (as does the hydroxyl of Ser27), it is more likely that the SH group of Cys27 would act as a donor to the water molecule. The resulting model was similar to that proposed for the ethanol-free D27S ecDHFR·MTX complex. Side-chain torsion angles for Ser27 and Cys27 are equivalent. However, the water molecules that are within hydrogen-bonding distance of the Oγ and Sγ atoms are not coincident since bonds to sulfur are longer than bonds to oxygen. In consequence, the water molecule in this D27C model is closer to MTX N8 while the analogous water molecule in the proposed D27S model is closer to MTX N1. Since the same number of hydrogen bonds are present, however, this comparison correlates with the similar values for $K_{d(MTX)}$ of the D27C and D27S mutants, as noted previously.

(*B*) *Case 2.* Alternatively, a model for ethanol-free D27C ecDHFR·MTX could be built with the Cys27 thiol group in the same position as seen in the crystal structure, facing Tyr151, and with water 806/808 hydrogen-bonded both to MTX and to the backbone carbonyl oxygen of Cys27 (see Figure 3). Water 806/808 could then accept hydrogen bonds from the MTX 2-amino and the Thr113 hydroxyl, and donate a hydrogen bond to the backbone carbonyl oxygen of residue 27. Another water molecule would probably then occupy the position of the ethanol oxygen atom observed in the crystal structure. However, this water would be weakly bound since there are no nearby protein hydrogen bond donors or acceptors. As in the model described above under case 1 for ethanol-free D27C·MTX, there are the same number of protein-mediated hydrogen bonds to MTX as in the proposed ethanol-free D27S·MTX complex.

At present, we cannot distinguish between these two possibilities for the geometry of the MTX-binding site of D27C in the absence of ethanol. However, we tend to favor case 1, with the cysteinyl SH closer to the binding site, as this geometry seems more consistent with the observed pH dependence of the kinetics of DHF reduction by D27C (see below).

D27C ecDHFR Kinetics. The change from aspartic acid to cysteine at residue 27 results in a decreased k_{cat} and increased $K_{m(DHF)}$ throughout the pH range measured (see Figure 2). Thus, at pH D27C has a k_{cat} that is 14-fold lower than wt, and $K_{m(DHF)}$ is 100-fold higher (see Table I). Compared to D27S at the same pH, D27C shows a 2-fold increase in $k_{cat}/K_{m(DHF)}$, with k_{cat} 5-fold higher and $K_{m(DHF)}$ increased by 2-fold. However, the pH profiles of the steady-state kinetic parameters for D27C differ markedly from D27S (see Figure 2). Most interestingly, the apparent pK_a of this mutant is shifted to values that are characteristic of the cysteine side chain (Creighton, 1983). The pH–activity profile pK_a values are, for log k_{cat}, 8.56 ± 0.02, and for log $[k_{cat}/K_{m(DHF)}]$, 9.64 ± 0.34. These pK_a's are to be compared with 8.4 and 8.1, respectively, in the wt profiles (Stone & Morrison, 1984). It is important to note, however, that the kinetic pK_a seen in the wt log k_{cat} vs pH profile reflects a change in the rate-limiting step from dissociation of THF from E·NADPH·THF to hydride transfer in E·NADPH·DHF (Fierke et al., 1987), whereas the pK_a seen in the D27C profile is probably an intrinsic value since primary deuterium isotope effects show hydride transfer to be rate-limiting throughout the pH range (see Table III). Thus, compared to the intrinsic pK_a of 6.5 for Asp27 in wt ecDHFR, the pK_a of D27C is shifted upward by 2 pH units. This observation implies that a protonated SH group of Cys27 contributes to the overall enzyme activity of the D27C mutant in somewhat the same manner as does a protonated Asp27 in the wt enzyme (see below).

Pre-steady-state stopped-flow experiments with D27C indicate that its hydride-transfer rate is about 100 times lower that for the wt enzyme. At pH 7.3, under single-turnover conditions, the observed rate constant for D27C is 1.7 ± 0.2 s^{-1}. As expected from the full deuterium isotope effect on ^DV noted above, the value of $k_{hydride}$ is within experimental error of the k_{cat}, 2.2 ± 0.16 s^{-1}, measured under steady-state conditions.

Compared to wt ecDHFR, and D27C mutation has slightly altered the binding of NADPH. The dissociation rate constant of NADPH from the binary complex is elevated 3-fold, while the association rate constant is unchanged from the wt (see Table II).

Mechanism of D27C ecDHFR and D27S ecDHFR. The activity vs pH behavior of D27C suggests that in the E·S complex the Cys27 thiol group resides near the DHF pteridine ring and is involved in substrate protonation. In contrast, the pH dependence of the enzymic activity of D27S suggests that a serine residue at this location cannot contribute to protonation of bound DHF since both k_{cat} and $k_{cat}/K_{m(DHF)}$ continue to decline sharply as the buffer pH is increased (see Figure 2). Why might a cysteine side chain contribute to protonation but not a serine side chain? A proton-relay circuit has been proposed (Bystroff et al., 1990) between Asp27 Oδ2, N3, and O4 of DHF and two bound water molecules to explain the ultimate protonation of DHF at N5. The thiol group of D27C may function in a similar manner as a surrogate for the Asp 27 Oδ2, albeit much less efficiently, in this proton-relay mechanism. Since a thiol group is much more easily ionized than a hydroxyl group, its proton is able participate in such a transient proton relay while the proton of the serine hydroxyl group cannot. At pH values above 8, where the thiol is ionized, this participation is no longer possible, hence, the observed kinetic pK_a for D27C.

Howell et al. (1986) have proposed that the kinetic activity of D27S is due to the mutant's binding of preprotonated DHF and the steep decline in activity with increasing pH is attributed to a decreasing concentration of protonated DHF in solution. The protonatable group on DHF is N5 which has a pK_a of 2.59 (Maharaj et al., 1990). In contrast, D27C exhibits a constant level of activity throughout the upper pH range (between pH 6.5 and 8.5), which is probably due to protonation of N5 by the enzyme, assisted by Cys27 as hypothesized above.

D27L ecDHFR

Preliminary steady-state kinetic analysis of another mutant, D27L ecDHFR, detected activity only at low pH (data not shown). At pH 5.0, k_{cat} was estimated to be 7.4×10^{-2} s^{-1}, and $K_{m(DHF)}$ was estimated to be 100 μM. D27L thus suffers a 280-fold decrease in k_{cat} and a 200-fold increase in $K_{m(DHF)}$, relative to wt. At pH values greater than 5, the mutant's enzymic activity was too low to measure accurately. These results suggest that this mutant cannot protonate DHF as well as wt, D27E, or D27C can, and cannot utilize preprotonated DHF as well as D27S can. Factors that may contribute to the low activity of D27L are its larger side chain size and increased hydrophobicity. The side-chain volume of leucine is 106.8 Å^3 compared to 51.0 Å^3 for aspartic acid.

CONCLUSIONS

Substitution of glutamic acid for Asp27 has produced a mutant enzyme that closely resembles wt ecDHFR with respect to structure, ligand binding, and kinetic mechanism. Although, as demonstrated by increased ligand dissociation rates, ground-state interactions between D27E and ligands are perturbed, the ability of the mutant to catalyze the chemical step in the reduction of DHF to THF has not been significantly compromised. By substituting cysteine for Asp27, we have, in effect, created a thiol-DHFR in which the cysteinyl SH group contributes to the mutant enzyme's ability to protonate the substrate. While k_{cat} is lower and $K_{m(DHF)}$ is higher in D27C than in the wt, this mutant is more efficient than D27S at catalyzing the reaction. These mutagenesis studies underscore the importance of the chemical nature of the proton-donating group at position 27 for catalysis.

ACKNOWLEDGMENT

We thank the San Diego Supercomputer Center for Cray time used to refine the D27C ecDHFR structure and Jay F. Davies, II, for help with refinement programs. We also thank J. Matthew Mauro, Mark Miller, Mark S. Warren, Michele A. McTigue, and Allen Gibbs for helpful discussions and Robert M. Aust for technical assistance.

REFERENCES

Adman, E., Watenpaugh, D. D., & Jensen, L. H. (1975) *Proc. Natl. Acad. Sci. U.S.A. 72*, 4854–4858.

Andrews, J., Fierke, C. A., Birdsall, B., Ostler, G., Feeney, J., Roberts, G. C. K., & Benkovic, S. J. (1989) *Biochemistry 28*, 5743–5750.

Baccanari, D. P., Daluge, S., & King, R. W. (1982) *Biochemistry 21*, 5068–5075.

Baker, D. J., Beddell, C. R., Champness, J. N., Goodford, P. J., Norrington, F. E. A., Smith, D. R., & Stammers, D. K. (1981) *FEBS Lett. 126*, 49–52.

Barshop, B. A., Wrenn, R. F., & Frieden, C. (1983) *Anal. Biochem. 130*, 134–145.

Beard, W. A., Appleman, J. R., Delcamp, T. J., Freisheim, J. H., & Blakely, R. L. (1989) *J. Biol. Chem. 264*, 9391–9399.

Bolin, J. T., Filman, D. J., Matthews, D. A., Hamlin, R. C., & Kraut, J. (1982) *J. Biol. Chem. 257*, 13650–13662.

Blakely, R. L. (1960) *Nature 40*, 1684–1685.

Blakely, R. L. (1984) in *Folates and Pterins* (Blakely, R. L., & Benkovic, S. J., Eds.) Vol. 1, pp 191–253, John Wiley & Sons, New York.

Bystroff, C., Oatley, S. J., & Kraut, J. (1990) *Biochemistry 29*, 3263–3277.

Cayley, P. J., Dunn, S. M. J., & King, R. W. (1981) *Biochemistry 20*, 874–879.

Charlton, P. A., Young, D. W., Birdsall, B., Feeney, J., & Roberts, G. C. K. (1979) *J. Chem. Soc., Chem. Commun, 20*, 922–924.

Chen, J.-T., Taira, K., Tu, C.-P. D., & Benkovic, S. J. (1987) *Biochemistry 26*, 4093–4100.

Cossins, E. A. (1984) in *Folates and Pterins* (Blakely, R. L., & Benkovic, S. J., Eds.) Vol. 1, pp 1–59, John Wiley & Sons, New York.

Creighton, T. (1983) in *Proteins, Structures and Molecular Principles*, W. H. Freeman & Co., New York.

David, C. L. (1992) Ph.D. Dissertation, University of California, San Diego, La Jolla, CA.

Davies, J. F., Delcamp, T. J., Prendergast, N. J., Ashford, V. A., Freisheim, J. H., & Kraut, J. (1990) *Biochemistry 29*, 9467–9479.

Dempsey, S. (1987) *Molecular Modeling System (MMS)*, Department of Chemistry Computer Facility, University of California, San Diego, La Jolla, CA.

Dreusicke, D., Karplus, P. A., & Schulz, G. E. (1988) *J. Mol. Biol. 199*, 359–371.

Dunn, S. M. J., & King, R. W. (1980) *Biochemistry 19*, 766–773.

Ellman, G. L. (1959) *Arch. Biochem. Biophys. 82*, 70–77.

Erickson, J. S., & Mathews, C. K. (1972) *J. Biol. Chem. 247*, 5661–5667.

Fierke, C. A., Johnson, K. A., & Benkovic, S. J. (1987) *Biochemistry 26*, 4085–4092.

Filman, D. J., Bolin, J. T., Matthews, D. A., & Kraut, J. (1982) *J. Biol. Chem. 257*, 13663–13672.

Freisheim, J. H., & Matthews, D. A. (1984) in *Folate Antagonists as Therapeutic Agents* (Sirotnak, F. M., Burchall, J. J., Ensminger, W. D., & Montgomery, J. A., Eds.) Vol. 1, pp 69–131, Academic Press, Inc., Orlando, FL.

Gregoret, L. M., Rader, S. D., Fletterick, R. J., & Cohen, F. E. (1991) *Proteins: Struct., Funct. Genet. 9*, 99–107.

Hendrickson, W. A., & Konnert, J. H. (1980) in *Computing in Crystallography* (Diamond, R., Ramaseshan, S., & Venkatesan, K., Eds.) pp 13.1–13.23, Indian Institute of Science, Bangalore, India.

Hermes, J. D., Morrical, S. W., O'Leary, M. H., & Cleland, W. W. (1984) *Biochemistry 23*, 5479–5488.

Hood, K., & Roberts, G. C. K. (1978) *Biochem. J. 171*, 357–366.

Howell, E. E., Villafranca, J. E., Warren, M. S., Oakley, S. J., & Kraut, J. (1986) *Science 231*, 1123–1128.

Howell, E. E., Warren, M. S., Booth, C. L., Villafranca, J. E., & Kraut, J. (1987) *Biochemistry 26*, 8591–8598.

Howell, E. E., Foster, P. G., & Foster, L. M. (1988) *J. Bacteriol. 170*, 3040–3045.

Howell, E. E., Booth, C., Farnum, M., Kraut, J., & Warren, M. S. (1990) *Biochemistry 29*, 8564–8569.

Huennekens, F. M., & Henderson, G. B. (1975) in *Chemistry and Biology of Pteridines* (Pfleiderer, W., Ed.) pp 179–196, Walter de Gruyter, Berlin.

Jones, T. A. (1978) *J. Appl. Crystallogr. 11*, 268–272.

Katti, S. K., Le Master, D. M., & Eklund, H. (1990) *J. Mol. Biol. 212*, 167–184.

Kaufman, B. T., & Gardiner, R. C. (1966) *J. Biol. Chem. 241*, 1319–1328.

Kerr, K. A., Ashmore, J. P., & Koetzle, T. F. (1975) *Acta Crystallogr. B31*, 2022–2026.

Kisliuk, R. L. (1974) in *Folate Antagonists as Therapeutic Agents* (Sirotnak, F. M., Ed.) pp 1–68, Academic Press, Orlando, FL.

Kistenmacher, T. J., Rand, G. A., & Marsh, R. E. (1974) *Acta Crystallogr. B30*, 2573–2578.

Kraut, J., & Matthews, D. A. (1987) in *Biological Macromolecules and Assemblies* (Jurnak, F. A., & McPherson, A., Eds.) Vol. 3, pp 1–72, John Wiley & Sons, New York.

Levitt, M., & Perutz, M. F. (1988) *J. Mol. Biol. 201*, 751–754.

London, R. E., Howell, E. E., Warren, M. S., Kraut, J., & Blakely, R. L. (1986) *Biochemistry 25*, 7229–7235.

Luzzati, V. (1952) *Acta Crystallogr. 5*, 802–810.

Maharaj, G., Selinsky, B. S., Appleman, J. R., Perlman, M., London, R. E., & Blakely, R. L. (1990) *Biochemistry 29*, 4554–4560.

Matthews, C. K., & Huennekens, F. M. (1960) *J. Biol. Chem. 235*, 3304–3308.

Matthews, D. A., Alden, R. A., Bolin, J. T., Freer, S. T., Hamlin, R., Xuong, N., Kraut, J., Poe, M., Williams, M., & Hoogsteen, K. (1977) *Science 147*, 452–455.

Matthews, D. A., Alden, R. A., Bolin, J. T., Filman, D. J., Freer, S. T., Hamlin, R., Hol, W. G. J., Kisliuk, R. L., Pastore, E. J., Plante, L. T., Xuong, N., & Kraut, J. (1978) *J. Biol. Chem. 253*, 6946–6954.

Matthews, D. A., Bolin, J. T., Burridge, J. M., Filman, D. J., Volz, K. W., Kaufman, B. T., Beddell, C. R., Champness, J. N., Stammers, D. K., & Kraut, J. (1985) *J. Biol. Chem. 260*, 381–391.

McGrath, M. E., Wilke, M. E., Higaki, J. N., Craik, C. S., & Fletterick, R. J. (1989) *Biochemistry 28*, 9264–9270.

McGregor, M. J., Islam, S. A., & Sternberg, M. J. E. (1987) *J. Mol. Biol. 198*, 295–310.
Morandi, C., & Attardi, G. (1981) *J. Biol. Chem. 256*, 10169–10175.
Murphy, D. J., & Benkovic, S. J. (1989) *Biochemistry 28*, 3025–3031.
Nakamura, H., & Littlefield, J. W. (1972) *J. Biol. Chem. 247*, 179–187.
Oefner, C., D'Arcy, A., & Winkler, F. K. (1988) *Eur. J. Biochem. 174*, 377–385.
Penner, M. H., & Frieden, C. (1985) *J. Biol. Chem. 260*, 5366–5369.
Poe, M., Greenfield, N. J., Hirshfield, J. M., & Hoogsteen, K. (1974) *Cancer Biochem. Biophys. 1*, 7–11.
Poe, M., Bennet, C. D., Donoghue, D., Hirshfield, J. M., Williams, M. N., & Hoogsteen, K. (1975) in *Chemistry and Biology of Pteridines* (Pfleiderer, W., Ed.) pp 51–59, Walter de Gruyter, Berlin.
Prendergast, N. J., Appleman, J. R., Delcamp, T. J., Blakely, R. L., & Freisheim, J. H. (1989) *Biochemistry 28*, 4645–4650.
Rossman, M. G., & Argos, P. (1975) *J. Biol. Chem. 250*, 7525–7532.
Schweitzer, B. L., Srimatkandada, S., Gritsman, H., Sheridan, R., Venkataraghavan, R., & Bertino, J. R. (1989) *J. Biol. Chem. 264*, 20786–20795.
Selinsky, B. S., Perlman, M. E., London, R. E., Unkefer, C. J., Mitchell, J., & Blakely, R. L. (1990) *Biochemistry 29*, 1290–1296.
Srinivasan, R., & Chacko, K. K. (1967) in *Conformation of Biopolymers* (Ramachandran, G. N., Ed.) Vol. 2, pp 607–615, Academic Press, London.
Stammers, D. K., Champness, J. N., Beddell, C. R., Dann, J. G., Eliopoulos, E., Geddes, A. J., Ogg, D., & North, A. C. T. (1987) *FEBS Lett. 218*, 178–184.
Stone, S. R., & Morrison, J. F. (1984) *Biochemistry 23*, 2753–2758.
Tartof, K. D., & Hobbs, C. A. (1987) *BRL Focus 9*, 12.
Thillet, J., Adams, J. A., & Benkovic, S. J. (1990) *Biochemistry 29*, 5195–5202.
Vanoni, M. A., & Matthews, R. G. (1984) *Biochemistry 23*, 5272–5279.
Villafranca, J. E., Howell, E. E., Voet, D. H., Strobel, M. S., Ogden, R. C., Abelson, J. N., & Kraut, J. (1983) *Science 222*, 782–799.
Viola, R. E., Cook, P. F., & Cleland, W. W. (1979) *Anal. Biochem. 96*, 334–340.
Volz, K. W., Matthews, D. A., Alden, R. A., Freer, S. T., Hansch, C., Kaufman, B. T., & Kraut, J. (1982) *J. Biol. Chem. 257*, 2528–2536.
Xuong, N., Freer, S. T., Hamlin, R., Nielson, C., & Vernon, W. (1978) *Acta Crystallogr. A34*, 289–295.

Registry No. Asp, 56-84-8; Glu, 56-86-0; Cys, 52-90-4; NADPH, 53-57-6; THF, 135-16-0; DHF, 4033-27-6; ethanol, 64-17-5.